

Assessing laser-tissue damage with bioluminescent imaging

Gerald J. Wilmink

Vanderbilt University
Department of Biomedical Engineering
5824 Stevenson Center
Nashville, Tennessee 37235

Susan R. Opalenik

Vanderbilt University
Department of Pathology and Department of
Veterans Affairs Medical Center
Nashville, Tennessee 37212

Joshua T. Beckham

Vanderbilt University
Department of Biomedical Engineering
5824 Stevenson Center
Nashville, Tennessee 37235

Jeffrey M. Davidson

Vanderbilt University
Department of Pathology and Department of
Veterans Affairs Medical Center
Nashville, Tennessee 37212

E. Duco Jansen

Vanderbilt University
Department of Biomedical Engineering
VU Station B #351631
Nashville, Tennessee 37235

Abstract. Effective medical laser procedures are achieved by selecting laser parameters that minimize undesirable tissue damage. Traditionally, human subjects, animal models, and monolayer cell cultures have been used to study wound healing, tissue damage, and cellular effects of laser radiation. Each of these models has significant limitations, and consequently, a novel skin model is needed. To this end, a highly reproducible human skin model that enables noninvasive and longitudinal studies of gene expression was sought. In this study, we present an organotypic raft model (engineered skin) used in combination with bioluminescent imaging (BLI) techniques. The efficacy of the raft model was validated and characterized by investigating the role of heat shock protein 70 (hsp70) as a sensitive marker of thermal damage. The raft model consists of human cells incorporated into an extracellular matrix. The raft cultures were transfected with an adenovirus containing a murine hsp70 promoter driving transcription of luciferase. The model enables quantitative analysis of spatiotemporal expression of proteins using BLI. Thermal stress was induced on the raft cultures by means of a constant temperature water bath or with a carbon dioxide (CO₂) laser ($\lambda=10.6\ \mu\text{m}$, 0.679 to 2.262 W/cm², cw, unfocused Gaussian beam, $\omega_L=4.5\ \text{mm}$, 1 min exposure). The bioluminescence was monitored noninvasively with an IVIS 100 Bioluminescent Imaging System. BLI indicated that peak hsp70 expression occurs 4 to 12 h after exposure to thermal stress. A minimum irradiance of 0.679 W/cm² activated the hsp70 response, and a higher irradiance of 2.262 W/cm² was associated with a severe reduction in hsp70 response due to tissue ablation. Reverse transcription polymerase chain reaction demonstrated that hsp70 mRNA levels increased with prolonged heating exposures. Enzyme-linked immunosorbent protein assays confirmed that luciferase was an accurate surrogate for hsp70 intracellular protein levels. Hematoxylin and eosin stains verified the presence of the thermally denatured tissue regions. Immunohistochemical analyses confirmed that maximal hsp70 expression occurred at a depth of 150 μm . Bioluminescent microscopy was employed to corroborate these findings. These results indicate that quantitative BLI in engineered tissue equivalents provides a powerful model that enables sequential gene expression studies. Such a model can be used as a high throughput screening platform for laser-tissue interaction studies. © 2006 Society of Photo-Optical Instrumentation Engineers. [DOI: 10.1117/1.2339012]

Keywords: bioluminescence; optical imaging; skin equivalents; laser-skin resurfacing; wound healing; CO₂ laser; hsp 70.

Paper 05301SSR received Oct. 7, 2005; revised manuscript received Feb. 28, 2006; accepted for publication Feb. 28, 2006; published online Aug. 31, 2006.

1 Introduction

Lasers play an increasing role in the medical field for diagnostic and therapeutic applications. Effective laser procedures are achieved by selectively tailoring the laser's parameters (wavelength, spot size, pulse duration, radiant energy, beam

profile) to the physical characteristics of the target tissue (anatomy, mechanical properties, heat capacity, thermal conductivity, absorption coefficient, scattering coefficient, anisotropy). Laser parameters are selected to optimize efficacy while minimizing unwanted side effects and tissue damage. From a phenomenological standpoint, it is known that laser-induced tissue injury occurs via oxidative, photothermal, pho-

Address all correspondence to E. Duco Jansen, Vanderbilt University, Department of Biomedical Engineering, VU Station B #351631, Nashville, TN 37235; Tel: 615-343-1911; Fax: 615-343-7919.

tomechanical, and photochemical mechanisms.¹ Nevertheless, the specific cellular and molecular pathways that initiate and govern these mechanisms remain poorly understood.^{1,2} Traditional efforts aimed at assessing cellular tissue damage have used postmortem strategies, such as histology, reverse transcription polymerase chain reaction (RT-PCR), *in situ* hybridization, and Western blots.^{3–6} The major shortcoming of these methods is that they all require sacrificing tissue, thereby precluding the ability to conduct sequential studies. Therefore, a strategy capable of reporting sublethal tissue damage in a noninvasive fashion was sought. Recent bioluminescent imaging (BLI) strategies have elucidated some of those signaling pathways that are activated during laser-induced tissue injury. The oxidative light emitting luciferase reaction of BLI can be harnessed for use as a surrogate marker for promoter activity. BLI has been used to monitor a variety of biological processes in wound healing, transplantation, and apoptosis.^{3,4,7–10} The key regulatory feature of BLI is accomplished by using the promoter sequence for the gene of interest, in our study heat shock protein 70 (hsp70), in conjunction with an optically active reporter, firefly luciferase (luc).

When tissue is thermally damaged, a cellular response mechanism consisting of heat shock proteins is activated. Heat shock proteins are employed to repair cellular damage and protect the cell from further thermal injury.¹¹ This heat shock response is dependent on both temperature and time and is induced by temperature increases of at least 5 to 6°C.^{11–13} Of the heat shock family members, the most highly inducible is hsp70.¹³ In the presence of cellular insults, hsp70 can be dramatically upregulated to make up to 15% of total cellular protein content.¹⁴ Due to its marked induction, hsp70 acts as a sensitive indicator of thermal damage to cells.^{6,13} Herein, the promoter sequence of the gene (murine hsp70a1) functions as an on-off switch for transcription of the light emitting luciferase. For this study, expression of the luc gene from the firefly (*Photinus pyralis*) was directed by the promoter of the hsp70 gene, as described previously.¹³ Thus, measuring the light emitted from the luciferase reaction using BLI strategies, provides a noninvasive method to quantify hsp70 transcription.

Besides the method of assessing tissue damage at the cellular level, selecting an appropriate study model also poses a formidable challenge. In comparable studies, human subjects have been used; however, using humans provides two intrinsic difficulties: (1) in measuring gene expression on a single subject over time and (2) in stringent medical limits (ethical and practical) of harvesting tissue samples at multiple times for histological and biochemical analysis.^{15,16} In light of these difficulties, animal models are used as a more viable model to study hsp70 expression and other laser-induced tissue effects.^{5,17} The porcine model is the closest nonprimate equivalent to human skin and is the most widely used dermal wound repair model, but because of differences in tissue architecture and immune responses, even it does not accurately reflect human wound healing.^{18,19} The use of cell cultures is an alternative to using human subjects and animal models, and we and others have successfully assessed hsp70 levels in cell culture.^{12,13} Cell culture studies provide valuable insights into the cellular response to thermal injury, but their utility is limited because cells, lacking an extracellular matrix (ECM), react differently than when incorporated in tissue. The ECM

provides skin with distinct thermal and optical properties, but also functions at a biochemical level to actively engage with the cell. In the 1980s, Bissell found that the ECM is a key “signaling molecule” crucial for the normal functioning of cells.²⁰ Consequently, models lacking an ECM, while providing useful information, do not accurately exhibit the cell-matrix relationship present in *in vivo* human skin.

Starting in the mid-1970s, many research efforts were focused on making multilayered skin equivalents. These organotypic tissue cultures became known as “raft” cultures and this method has been further modified for skin and other tissue applications.^{15,16,21} Skin raft cultures are human skin equivalents comprised of stromal and epithelial layers. The stromal layer is composed of human fibroblasts in a collagen matrix. Human keratinocytes are grown atop the dermal equivalent, and once transferred to a liquid-air interface differentiate akin to that observed in *in vivo* human skin.²² Herein, we employed raft cultures as our model because they are more easily available and more reproducible than samples derived from human subjects, consist of all human cells, and provide information regarding cell-matrix interactions.

In this study, we sought to develop a model that emulates human tissue while providing us with the capability of noninvasively, quantitatively, and sequentially assessing sublethal thermal damage. Our model employs a raft culture that has been equipped with a heat-inducible reporter gene system to assess the heat shock response using BLI. This model was developed, characterized, and validated using a heated water bath and a CO₂ laser using parameters similar to those used in laser skin resurfacing (LSR). The CO₂ laser is the criterion standard for LSR because it can be manipulated in such a fashion, to control the depth of epidermal vaporization while eliciting minimal damage to the papillary dermis.²³ The infrared wavelength is highly absorbed by tissue, which consists primarily of water and collagen, and minimizes residual thermal damage (RTD).^{24,25}

The overall goals of this study are (1) to develop an organotypic skin raft model, transfected with a hsp70-luc reporter gene construct to study spatiotemporal trends of hsp70 expression using BLI strategies, (2) to validate the use of BLI as a surrogate marker for hsp70 expression by correlating BLI with conventional methods of hsp70 analysis, and (3) to demonstrate feasibility of this approach with a heated water bath and with clinically relevant CO₂ laser parameters.

2 Materials and Methods

2.1 Cell Culture Conditions

Normal human neonatal dermal fibroblast (NHDF), normal human epithelial neonatal foreskin keratinocyte (NHEK), and normal human epithelial melanocyte (NHEM) (medium pigment) primary cell lines were obtained from the Vanderbilt University’s Skin Diseases Research Core Center (SDRCC). The NHDFs were cultured in Dulbecco’s Modified Eagle’s Medium (DMEM) and supplemented with 10% fetal bovine serum (FBS), (GIBCO BRL, Gaithersburg, Maryland). The NHEKs were cultured in Epilife Media, 1% human keratinocyte growth supplement—V2 (HKGS-V2), 1% penicillin-streptomycin-amphotericin B (PSAB) (Cascade Biologics, Inc., Portland, Oregon). The NHEMs were cultured in medium 154 calcium-free (CF) media, 1% human melanocyte

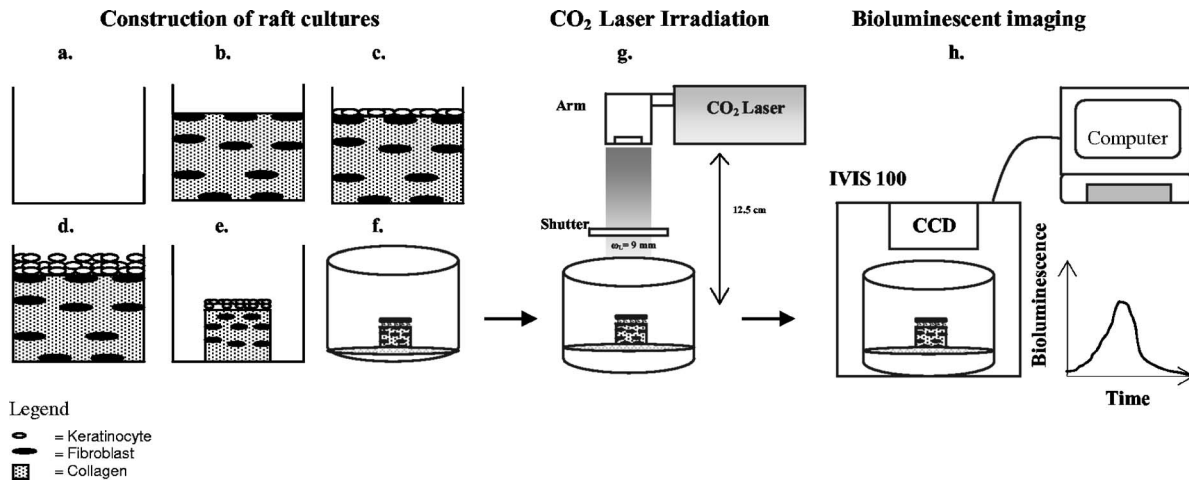


Fig. 1 Schematic representation of experimental methodology. Construction of organotypic raft cultures: (a) In a 24 well plate. (b) NHEKs were mixed in a collagen matrix. (c) NHEKs were added on top of each raft. (d) NHEKs begin to differentiate. (e) The NHEKs induced contraction of rafts. (f) Rafts were lifted to air-liquid interface in petri dish and NHEKs fully differentiated after 10 to 14 days. (g) Mature rafts were transfected with 100 μ l (MOI=1.0) of Ad-hsp70-luc and irradiated with CO₂ laser with irradiances from 0.679 to 2.262 W/cm² for 1 min. (h) The bioluminescent signal was captured with an IVIS-100 or 200 BLI system.

growth supplement (HMGS), and 1% PSAB (Cascade Biologicals, Inc.). All cells were incubated at 37°C and 5% CO₂ under humidified conditions.

2.2 Recombinant Adenovirus Construction

Briefly, the Ad-hsp70a1-luc-IRES-eGFP was constructed as follows. The hsp70-luc construct was provided courtesy of Dr. Contag (Stanford University) and consisted of a mouse hsp70a1 promoter (95% homology to human hsp70A1A) with a truncated firefly luciferase gene (luc+) inserted downstream as described previously.^{12,13,26} The hsp70-luc cassette was subcloned into a modified pShuttle vector (Qbiogene, Morgan Irvine, California) upstream of an IRES-eGFP cassette.¹⁰ Generation of the final Adv construct was performed by cotransformation of the pShuttle-hsp70-luc-IRES-eGFP with the pAdEasy1 adenoviral vector by homologous recombination in *E. coli* as per manufacturer's instructions (AdEasy, Qbiogene).

Recombinants were selected for kanamycin resistance and confirmed by restriction endonuclease analysis. The final linearized Adv construct was transiently transfected into 293 cells to produce infectious virus particles (Superfect, Qiagen, Valencia, California).

2.3 Virus Propagation and Purification

Following lysis and purification, the adenovirus had a titer of 1.3×10^7 plaque forming units (PFU)/ml. The multiplicity of infection (MOI) is defined as the ratio of number of infectious virus units (PFU) to the number of cells. The transfection efficiency was optimized (data not shown), and the results demonstrated that a MOI of 1 generated the best response while minimizing virus use.

2.4 Construction of Organotypic Raft Cultures

Organotypic raft cultures were constructed essentially as described,^{16,21} with the concentration of NHEKs increased to 6×10^6 cells/ml. A schematic illustrating raft construction is

provided in Figs. 1(a)–1(f). The raft cultures were incubated for 10 to 14 days in an atmosphere of 37°C, 5% CO₂, and media was changed every other day. Typical rafts were ~10 mm in diameter and ~2-mm thick. After this incubation period, the rafts were transfected with the Adv-hsp70-luc at a MOI of 1 and incubated for 15 h. Once transfected, the rafts were washed with phosphate buffered saline (PBS), and then exposed to heat shock conditions. The heat shock conditions were provided by a constant temperature water bath or by a CO₂ laser.

2.5 Water Bath and Laser Irradiation Experiments

2.5.1 Cell culture experiments

In order to understand the individual contribution that each cell type has to the raft model, cell culture experiments were conducted to characterize the heat shock response of the cell line. On day 1, the cells were plated in six well (9.62 cm²) tissue culture plates with 9.6×10^4 cells per well in 2 ml of culture medium (Costar, Fisher Scientific, Sewanee, Georgia). For the enzyme-linked immunosorbent assay (ELISA) experiments, 2.5×10^5 cells per well were used to ensure adequate protein levels. After 24 h, the cells were transfected with the adenovirus and returned to a 37°C, 5% CO₂ incubator (Forma Scientific, Marietta, Ohio) for ~15 h. After incubation, the transfection media was aspirated and the cells were washed with PBS. Fresh media were added to the cells, the culture plates were sealed with parafilm to prevent contamination, and then heat shocked by floating them in a water bath at 43°C or 44°C for varying exposure times (0 to 40 min). The maximum exposure time of 40 min at 44°C was selected based on previous hsp70 studies.¹³ Heat shocked cells were placed back in a 37°C, 5% CO₂ incubator (Forma Scientific). Bioluminescent images were taken of the cells as described below.

2.5.2 Water bath and laser radiation experiments of raft cultures

Transfected raft cultures were exposed to a heated water bath or to CO₂ laser radiation. For each experiment, two controls were included to account for background luciferase activity (normally <0.01% of BL signal) and for constitutive hsp70 expression. The first control was a raft that was not transfected or heat shocked, and the second control was a raft that was transfected but not heated. Comparable water bath conditions were applied to the rafts as described in Sec. 2.5.1.

2.5.3 CO₂ laser irradiation

The ablating laser used in this study was a cw CO₂ laser ($\lambda = 10.6 \mu\text{m}$, Laser Industries, Sharplan 1060, Tel Aviv, Israel). The laser beam profile was measured to be Gaussian by pin-hole measurements. The laser beam radius was selected to ensure full raft radiation. A collimated beam with a radius (ω_1) of 4.5 mm was delivered to the raft cultures via an articulated arm. The laser parameters selected for this experiment ensured that the entire raft's area was radiated, but due to the inherent Gaussian beam profile, the center of the raft experienced the highest irradiance. An external shutter (VMM-T1, Vincent Associates, Rochester, New York) was placed 2.5 cm below the fixed arm. The external shutter was used to control laser exposure time. A schematic illustrating the laser setup is provided in (Fig. 1(g)).

2.5.4 Inducing hsp70 expression with the laser

Studies by Beckham et al. showed that the expression of hsp70 follows an Arrhenius-type rate process, suggesting that hsp70 expression levels depend not just on temperature but on the temperature-time history.¹³ Studies investigating hsp70's temperature-time history have observed that maximal hsp70 expression occurs in cells for minute exposures at temperatures ranging from 50 to 64.6°C.¹² Using a thermocouple, the irradiances of 0.679 to 2.262 W/cm² for 1 min exposures, as used in our experiments, were confirmed to generate comparable temperatures 500 μm below the surface of each raft (data not shown).

2.6 BLI

Prior to BLI, the substrate for the bioluminescence reaction, *D*-luciferin potassium salt (Biosynth AG, Switzerland) in double distilled H₂O at a stock concentration of 0.94 mg/ml was administered to each sample. For the cell experiments, 100 μl of stock substrate was delivered to 2 ml of growth media per well, resulting in a final substrate concentration of 0.047 mg/ml. For raft experiments, 200 μl of substrate was delivered to each raft. After delivery of the substrate, the cells and raft cultures were incubated for 1 min before imaging to ensure maximal bioavailability of the substrate while accounting for the half-life of luciferase.²⁷

2.6.1 BLI system

The luciferase-induced bioluminescent light emission was measured at various time points following heat shock using an IVIS 100 bioluminescent imaging system (Xenogen, Alameda, California). Culture plates containing rafts or cell cultures were placed in the imaging chamber on a heated 37°C stage and were imaged. Both photographic and biolu-

minescent images were acquired. The bioluminescent image was then superimposed on top of the photographic image. The bioluminescent data is represented with a false color scheme representing the regions of varying light emission. The light emission was quantified using Living Image analysis software (v2.12, Xenogen). The light emission from specified regions of interest (ROIs) was quantified as a photon flux in units of the total number of photons emitted/second/ROI ($p/s/\text{ROI}$).

2.6.2 BLI of cell cultures

For all cell culture experiments, the bioluminescent signal was acquired for a seeding density of 9.6×10^4 cells/well in a six well plate. For each experiment, a negative control (transfected cells, no heat shock) was employed. The experimental group consisted of cells that were exposed to heat shock conditions. After the experimental cells were heat shocked, both sets of cells were imaged in the same manner. Substrate (100 μl) was readministered to the cells 1 min before each imaging point. Images were collected at 0, 2, 4, 6, 8, 12, 24, and 48 h after the start of the heating protocol. Bioluminescence images were integrated over 3 min.

2.6.3 BLI of laser irradiated raft cultures

To investigate the bioluminescent intensity of adenovirally transfected raft cultures in response to heating with a dermal laser (CO₂), 28 rafts were constructed and allowed to differentiate for 12 days. On day 12, the rafts were transfected with 100 μl of adenovirus (MOI=1.0) and incubated for 15 h. The 28 rafts were divided into 7 groups of 4 and included 2 negative control groups ($n=4$), with 1 group with no adenovirus and no heat shock and the other with adenovirus and no heat shock. The third group was a positive control ($n=4$), which consisted of samples that were heated in a water bath at 44°C for 20 min. The final four groups were exposed to laser radiation from a cw CO₂ laser ($n=4$ for each). These groups were irradiated with 0.43, 0.72, 1.0, and 1.43 W of power, respectively, with corresponding irradiances of 0.679, 1.131, 1.584, and 2.262 W/cm² for 60 s. For each raft culture, the bioluminescent images were acquired as described above. The ROI was defined as the area corresponding to one raft. Because more cells are present in a raft than in one well, more substrate was delivered to the rafts before imaging. Two hundred microliters of substrate was delivered to each raft before imaging by pipetting the substrate directly on to the rafts. Images were integrated over 1 min.

2.7 ELISA Assays

In order to correlate photon counts from imaging to actual hsp70 production in each of the cell types, an ELISA kit EKS-700 was used to quantify hsp70 protein levels in the samples (Stressgen, Victoria, British Columbia, Canada).

For this experiment, the NHDF, NHEM, and NHEK cell lines were seeded in six-well plates at a concentration of 2.5×10^5 cells per well, transfected (MOI=1) and incubated overnight. Fifteen hours later, the transfection media was aspirated, and the cells were washed with PBS. Fresh media was added to the cells and the cells were heat shocked at 44°C for 20, 30, and 40 min. One hundred microliters of substrate was added to the cells. The cells were imaged 12 h after heat

shock induction with the IVIS system. After imaging, the cells were lysed and the ELISA was conducted according to supplier's instructions (Stressgen).

2.8 RNA Preparation and Real-Time RT-PCR Analysis

To determine mRNA levels of hsp70, RNA was extracted from the cells that were exposed to water bath heating (44°C for 10, 20, and 40 min) and assessed by real-time RT-PCR. RNA was harvested from cell cultures with the RNeasy kit according to manufacturer's instructions (Qiagen). One microgram of each sample was DNase and reverse transcribed into single stranded cDNA with a high capacity cDNA archive kit using random primers according to manufacturer's instructions (Qiagen and ABI, Foster City, California). cDNAs were used as template in duplex PCR reactions, whereby amplification of the housekeeping gene, β -actin, is performed in the same reaction tube with that for hsp70. β -actin was selected as the endogenous control because under heat shock conditions, β -actin had the smallest intrasample variability (student *t* test, $p=0.55$) compared to glyceraldehyde-3-phosphate dehydrogenase and 18S (data not provided). Each PCR reaction contained 5 μ L of cDNA template (50-ng RNA equivalent), 10 μ L of 2 \times TaqMan PCR Master Mix (ABI), 1 μ L of β -actin 20 \times Gene Expression Assay-VIC (ABI), 1 μ L of HSPA1A 20 \times Gene Expression Assay-FAM (ABI), and 3 μ L of water. The cycling PCR reactions were performed in the iCycler, iQ machine (Bio-Rad, Hercules, California) and consisted of a 10-min hot start at 95°C followed by 40 cycles of 95°C denaturation for 15 sec and 60°C annealing/elongation for 1 min. Relative quantitation of mRNA levels were assessed using the comparative C_T method.²⁸ The hsp70 expression from each sample was normalized to β -actin and calculated as a fold induction compared to control. The control for each cell type was a sample that was not heat shocked and was extracted at time=0.

2.9 Flow Cytometry

In order to provide information to supplement the ELISA data, cell viability and apoptosis assays were performed using flow cytometry. As described in Sec. 2.7, at 12 h after thermal stress, medium was removed, then cells were trypsinized and resuspended in PBS, and stained for 45 min for viability using Molecular Probes' LIVE/DEAD viability and cytotoxicity stain (L-3224, Invitrogen Corporation, Carlsbad, California) containing calcein acetoxymethyl ester (stains live cells green) and ethidium homodimer-1 (stains membrane compromised cells red). The cells were similarly analyzed for early signs of apoptosis using JC-1 stain from Molecular Probes, MitoProbe JC-1 Assay Kit (M34152). All cells were analyzed using a flow cytometer and counted with a Coulter counter (FACS-Calibur, Becton Dickinson, Franklin Lakes, New Jersey, and Beckman Coulter Counter).

2.10 Histology and Immunohistochemistry

A subset of raft cultures were harvested for immunohistochemical analysis in order to examine raft tissue architecture, to spatially correlate the hsp70 protein expression to luciferase expression, and to examine conventional histological markers of thermal damage. Twelve hours after laser irradiation (which is the point at which maximum hsp70 expression

has been observed), the raft cultures were fixed in Tellyesniczky/Fekete solution (70% ethyl alcohol, glacial acetic acid, 37 to 40% formalin) or flash frozen in liquid nitrogen. The samples were sectioned at 7 μ m and stained. Histological analyses consisted of hematoxylin and eosin (H&E) and Gomori's trichrome (green) stains.²⁹ Immunohistochemical localization of hsp70 was conducted using mouse monoclonal hsp70 antibody (Santa Cruz Biotechnology, Santa Cruz, California), diluted 1:200. The application of the Envision+HRP system (DakoCytomation, Carpinteria, California) and DAB+ produced visible, interpretable results.

2.11 Bioluminescent Microscopy

Bioluminescent microscopy was conducted to examine the spatial distribution of *in situ* adenoviral transfection and to examine the hsp70-mediated luciferase expression throughout the raft. Samples were embedded in optical cutting temperature (OCT), flash frozen in liquid nitrogen and sectioned with a microtome (96- μ m thickness). Cross sections of the rafts were placed on a frozen microscope slide. A combination of 10 mM of adenosine triphosphate (500 μ l) and 0.94 mg/ml of luciferin (100 μ l) were delivered to the slice and imaged for 1 min with the IVIS 200 imaging system (Xenogen). The IVIS 200, unlike the IVIS 100 that is used in all other experiments, is equipped with a custom-made high magnification lens giving a distortion-free field of view of 3.9 cm. Combined with a binning of 1 and the enlarged chip size (2048 \times 2048 pixels), this allows for imaging with a resolution of 20 to 60 μ m, depending on the *f*-stop.

2.11.1 *In situ* raft transfections with Ad-CMV-luc

To address the question whether *in situ* transfection would indeed result in a spatially homogenous transfection in raft cultures, we used an adenovirus that expressed luc under control of a constitutive cytomegalovirus (CMV) promoter (Ad-CMV-Luc-IRES-GFP).¹⁰ Rafts were transfected with Ad-CMV with a MOI=1 for 15 h and then washed with PBS. Forty-eight hours after transfection (the point corresponding to maximum expression for this construct), the rafts were imaged and then harvested for bioluminescence microscopy.

2.11.2 Colocalizing luciferase expression to hsp70 expression

In order to colocalize the hsp70-induced luciferase expression (i.e., bioluminescent light emission) to actual hsp70 protein, a transfected raft [Ad-hsp70-luc (MOI=1)] was irradiated with the CO₂ laser (1.584 W/cm² for 1 min). Twelve hours after laser radiation (the point corresponding to maximum hsp70 expression), the rafts were imaged and then harvested for bioluminescence microscopy.^{12,13}

3 Results

3.1 Bioluminescence of hsp70-Driven Luciferase in NHDFs

Figure 2 shows the results of transfected fibroblasts (MOI of 1) that were heat shocked 15 h after transfection. Cells were exposed to a water bath of 43 or 44°C for 10, 20, or 40 min. Bioluminescent intensity was acquired 0, 2, 4, 6, 8, 10, 12, and 24 h after heat shock. The results indicate that

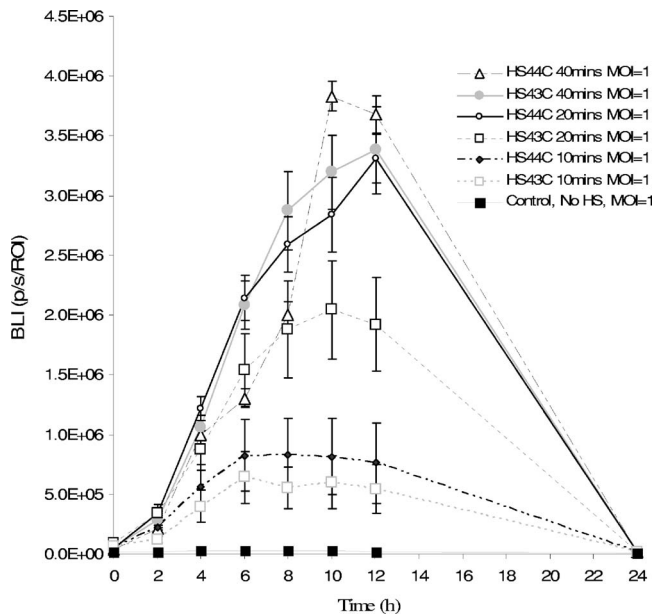


Fig. 2 Bioluminescent intensity for NHDFs transfected with Ad-hsp70-luc plotted over time. Maximal hsp70 expression occurred 8 to 12 h after heat shock. This experiment included seven groups conducted in triplicate: unheated control, heat shocked at 43°C for 10 min (hereafter, HS43°C-10 min), HS43°C-20 min, HS43°C-40 min, HS44°C-10 min, HS44°C-20 min, and HS44°C-40 min. All samples were seeded with NHDFs at a concentration of 9.6×10^4 cells per well. At $t = -15$ h, the NHDFs were treated with a Ad-hsp70-luc with a MOI of 1. One hundred microliters of *D*-luciferin (0.94 mg/ml) was added to each well 1 min before the NHDFs were imaged. Error bars represent the standard deviation for each group.

maximal hsp70 expression occurs 8 to 12 h after heat shock. Moreover, relative to the non-heated control, hsp70-driven luciferase is induced as much as 160-fold. Similar to previously published results in stably transfected cells, the trend suggests the severity of the heat shock is directly proportional to the magnitude of the heat shock response.¹³

3.2 Transcriptional and Translational Profiles for Skin Cells

The goal for this experiment was to examine the hsp70 response for three skin cell lines (NHDFs, NHEKs, and NHEMs) at five conditions (10, 20, 30, and 40 min at 44°C, and an unheated control) using the following assessment tools: bioluminescence, native hsp70 protein levels, cell viability, and real-time RT-PCR. Figures 3(a)–3(c) show the bioluminescence intensity plotted versus the heating protocols, Figs. 3(d)–3(f) show the bioluminescence plotted versus the native hsp70 protein levels (as quantified using ELISA), and Figs. 3(g)–3(i) show the percent of viable and apoptotic cells (as quantified using flow cytometry with JC-1 assay) of the three cell types. Data reported is 12 h post-heat shock. Figures 4(a)–4(c) show the relative hsp70 mRNA fold induction compared to control relative to β -actin versus time.

For all cell types, statistically significant ($P < 0.05$) increases in bioluminescent intensity are observed with increasing times of heat exposure [Figs. 3(a)–3(c)]. The peak bioluminescent intensities for the NHDFs and the NHEMs are comparable (both $\sim 10^8$ photons/s), while the NHEKs peak

bioluminescent intensity is observed to be 10 times higher. In Fig. 3(d)–3(f) it is observed that as the bioluminescent intensity is increased the native hsp70 protein levels are linearly increased ($R^2 > 0.96$), except for the NHEMs where no clear relationship exists. The data in Fig. 3(g) and 3(h) reveals for the NHDF and NHEK, at all heating exposures, less than 30% of the cells demonstrate early signs of apoptosis. Apoptotic levels were not statistically different from unheated controls. Conversely, Fig. 3(i) shows that the NHEMs, at all heating exposures, including the unheated controls, have greater than 60% of their cells being apoptotic.

For all cell types, statistically significant ($P < 0.05$) increases in hsp70 mRNA are observed with increasing times of heat exposure [Figs. 4(a)–4(c)]. Peak hsp70 mRNA expression occurred for all cells at 4 to 6 h after heat shocking. Maximal mRNA levels occurred 4 h after heat shocking for the NHDFs and the NHEMs, and at 6 h for the NHEKs. For all cell types, lower heating protocols (HS 44°C 10 mins) resulted in a quicker mRNA response (~ 0 to 4 h), while higher heating protocols (HS 44°C 40 mins) had maximal mRNA transcription at 6 h. The maximal hsp70 mRNA fold induction of 725 times that of the control occurred in the NHDFs 4 h after heat shocking.

3.3 Transfection is Cell-Type Dependent

To determine cell-type specific heat shock responses, the intracellular hsp70 protein levels and bioluminescent intensity were observed at various heating exposures. These tests were conducted to determine if the cell types exhibited different protein and luminescence levels for the same amount of delivered transgene. Figure 5(a) shows the measured protein levels (from ELISA assay) plotted versus increasing heat exposures. For all cell types, except the NHEMs, as the heating exposure is increased the hsp70 protein concentration increases. The NHDFs and NHEKs show similar hsp70 protein levels per given heating protocol, with the NHDFs expressing slightly higher, and statistically significant ($P < 0.05$) more hsp70 than the NHEKs. In contrast, the NHEMs' hsp70 protein concentration decreases as exposure to heat shock conditions increases.

For the three cell types, the bioluminescent intensity is plotted versus increasing heat exposures [Fig. 5(b)]. Increasing the heating time increases the bioluminescent intensity for all cell types. However, the keratinocytes produce a factor of 9 to 10 times more bioluminescence for a given heating protocol compared to fibroblasts. For example, when comparing fibroblasts and keratinocytes heated for 30 min, the luminescent intensity of the keratinocytes is approximately 10 times higher than that produced by the fibroblasts, despite the fact that hsp70 protein levels, as well as the hsp70 mRNA levels in both cell types are similar.

3.4 Transient Transfections

The expression of transgenes delivered by means of adenovirus has been reported to decrease over time due to extrusion of viral DNA and cell division, both of which lower the content of viral DNA per cell.³⁰ It should be noted that adenoviral transfection, despite a number of advantages, including high transfection efficiency, is particularly vulnerable to this because the transgene remains episomal and does not integrate

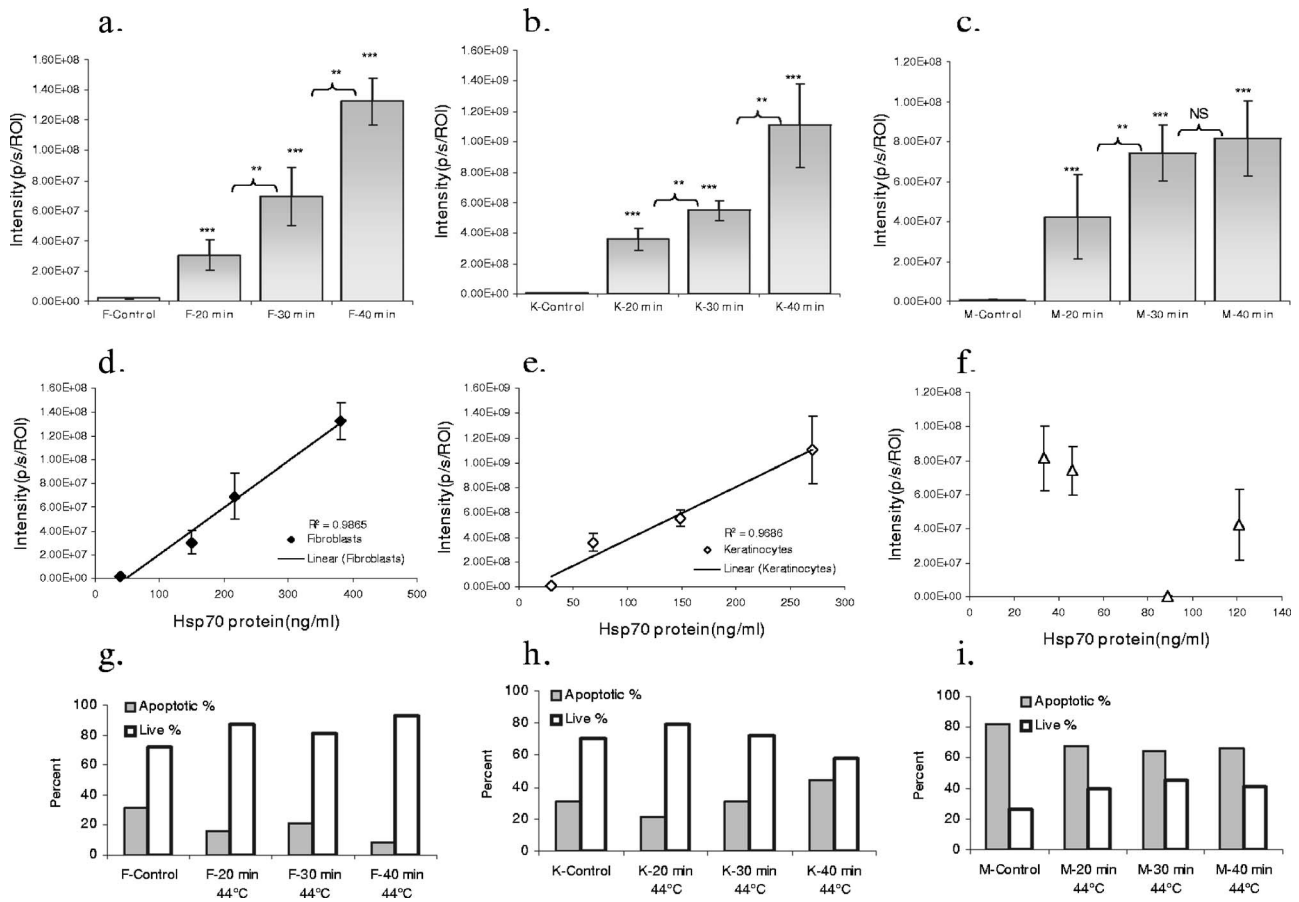


Fig. 3 Characterizing the hsp70 response in NHDF, NHEK, and NHEM cell lines. Bioluminescence for NHDF (a), NHEK (b), and NHEM (c); ELISA for NHDF (d), NHEK (e), and NHEM (f) and JC-1 apoptosis assay for NHDF (g), NHEK (h), and NHEM (j). For all cell types, increasing the heating protocol results in increased bioluminescence. Bioluminescence intensity and hsp70 protein levels are linearly correlated for the fibroblasts ($R^2 = 0.987$) and keratinocytes ($R^2 = 0.969$), but not for the NHEMs. More than 60% of the NHEMs showed early signs of apoptosis. For each cell type, 2.5×10^5 cells/well were plated in 4 six-well plates. A control for each cell type consisted of cells that were transfected, but not heat shocked. All cells were transfected with Ad-hsp70 with a MOI of 1 for ~ 15 h and then heat shocked in a water bath at 44°C for 20, 30, and 40 min. Twelve hours after heat shock, $100 \mu\text{l}$ of *D*-luciferin (0.94 mg/ml) was added to each well 1 min before the cells were imaged for bioluminescence. An ELISA for actual hsp70 protein levels was then conducted on each sample. The JC-1 expression (early apoptotic signal) for each sample group was analyzed using flow cytometry. The mean and standard deviations for bioluminescent intensities were statistically compared using a student's *t*-test (** $^* = P < 0.001$, ** $= P < 0.05$, $= P < 0.01$, and $n = 4$).

into the genomic DNA. In light of the fact that construction of a raft skin equivalent typically takes 10 to 14 days, we aimed to discern whether our system experiences a decrease in transgene expression, which would ultimately preclude us from transfecting our cells before constructing our raft cultures.²¹ We seeded 9.6×10^4 NHDF cells/well in 7 six-well plates. At $t = 0$, all cells were transfected (Adv-hsp70-luc) and incubated for 15 h. The media was changed for all plates, and at $t = 15$ h, the first plate was heated at 44°C for 40 min. Ten hours later ($t = 25$ h), the plate was imaged. The second plate was heated 24 h after the first plate ($t = 39$ h) and imaged 10 h later at ($t = 49$ h). This process was repeated for the remaining plates. The results are shown in Fig. 6(a) and demonstrate that transgene expression decreases over time. The bioluminescent intensity sharply increased from 0 to 49 h and decreased from 49 to 145 h. The third point, 49 h after transfection, had the highest bioluminescent intensity. From 49 to 72 h, a 50% decrease of bioluminescent signal was observed.

At $t = 145$ h, the signal decreased to less than 17% of the initial signal, 25 h postinfection.

From these results, we concluded that transfecting cells prior to construction of a raft (which take 10 to 14 days for maturation) is not feasible due to the fact that by the time the raft is fully stratified, very little transgene expression remains. For the remainder of the experiments, we first constructed each raft (as described in Sec. 2.4) and then ~ 15 h prior to heat shock treatment, transfected the rafts *in situ* in the petri dish by applying $100 \mu\text{l}$ of adenovirus (MOI=1) directly onto the rafts.

3.5 Homogeneously Transfecting Rafts In Situ

In order to ensure that our *in situ* raft transfections were homogenous, rafts were assessed using standard BLI strategies and bioluminescent microscopy. For this study, a mature raft

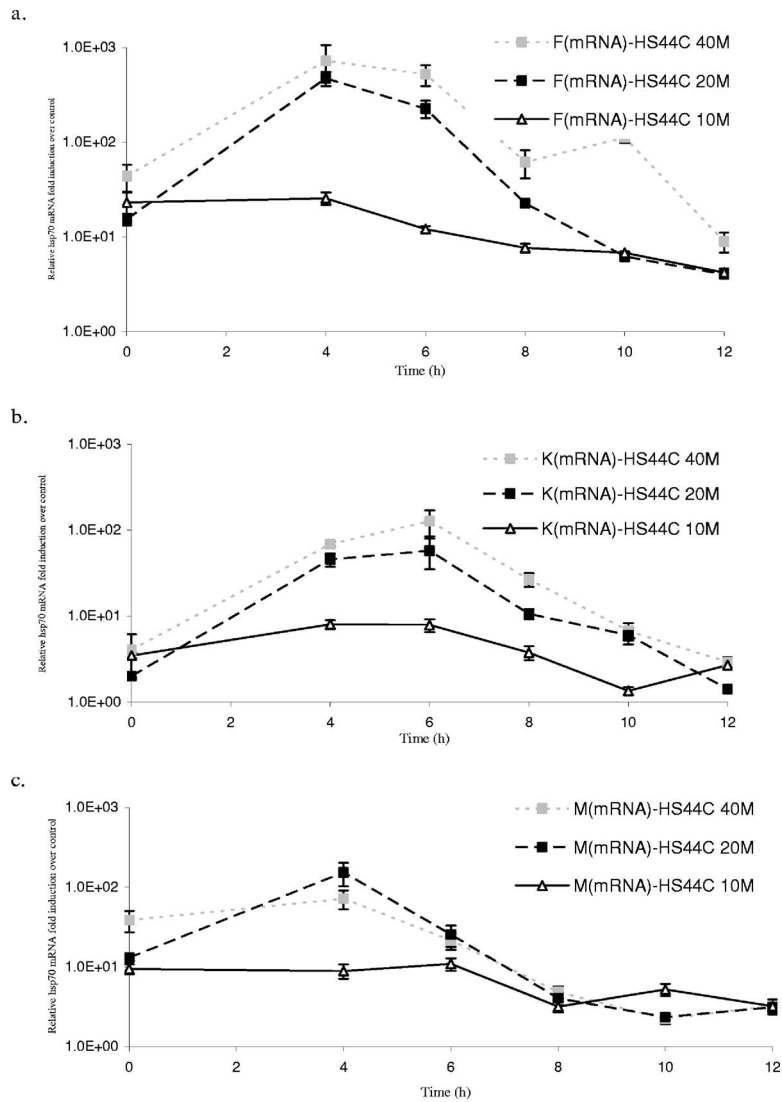


Fig. 4 Measuring hsp70 mRNA expression with real-time RT-PCR in NHDFs (a), NHEKs (b), and NHEMs (c). A total of 2.5×10^5 cells/well were plated in six-well plates and transfected with Ad-hsp70-luc (MOI=1). The cells were then heat shocked in a water bath at 44°C for 10, 20, and 40 min. After heat shocking, the total RNA was isolated, and 1 μ g of RNA from each sample was reverse transcribed into single-stranded cDNA. Real-time, duplex PCR was performed to examine hsp70A1A (FAM), and the endogenous control, β -actin (VIC). Relative quantitation of mRNA levels was assessed using the comparative C_T method. The hsp70 mRNA expression from each sample was normalized to β -actin and evaluated relative to controls. The final hsp70 mRNA expression was calculated as a fold induction compared to control.

transfected with constitutively expressed Ad-CMV-luc (MOI=1) was imaged 48 h after transfection [Fig. 6(b)]. The bioluminescent intensity is provided in Figs. 6(c) and 6(d), and the homogeneity of the transfections was demonstrated laterally (*X* and *Y*) and in cross section (*X* and *Z*). The lateral image revealed that $\sim 10^8$ (*p/s*) was recorded across the entire raft. The bioluminescent microscopy image of the same raft showed that a constant $\sim 2 \times 10^6$ (*p/s*) was emitted across the entire raft. The consistent bioluminescent intensity in the *xy* and *xz* planes indicated an effective homogenous transfection *in situ*.

3.6 Bioluminescence of Laser Irradiated Raft Samples

The bioluminescent intensity is plotted versus time for the following raft samples: laser irradiated with 1.584 W/cm² for 60 s, water bath heated at 44°C for 20 min, and the unheated

control [Fig. 7(a)]. Figure 7(b) shows the quantitative bioluminescence intensity plotted over time for all of the samples. The bioluminescence intensity is normalized by dividing the sample average bioluminescence intensity by the unheated controls average bioluminescence intensity. This *fold-increase* value in bioluminescence illustrates the increase in bioluminescent signal that occurs due to heat-inducing conditions. For all laser irradiated samples, the maximal expression occurred at *t*=4 to 8 h after exposure. Maximal expression occurred at *t*=4 h for the rafts heated in a water bath. The rafts exposed to a power of 1.0 W (1.584 W/cm²) had the highest bioluminescent expression. Rafts irradiated with the highest irradiance (2.262 W/cm²) were almost completely ablated and, hence, had few viable cells left to contribute to the bioluminescence signal.

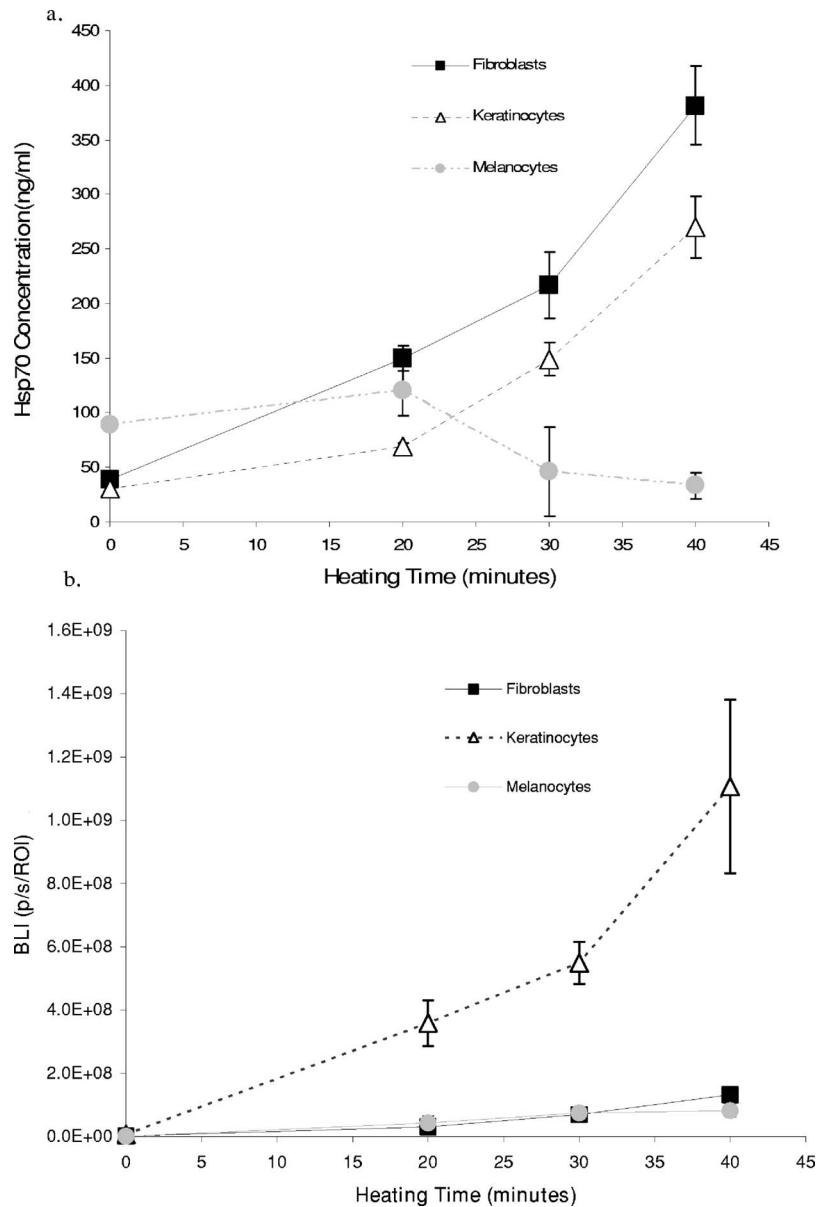


Fig. 5 Hsp70 protein concentration (a) and bioluminescent intensity (b) plotted versus heating time. For all cell types, except the NHEMs, as the heating exposure is increased, the hsp70 protein concentration increased. The NHEKs, produce one order of magnitude more bioluminescence for a given heating protocol compared to the NHDFs and NHEMs. For this experiment, each cell type was plated in 4 six-well plates at a concentration of 2.5×10^5 cells/well. A control for each cell type consisted of cells that were transfected, but were not heat shocked. All cells were transfected with Ad-hsp70 with a MOI of 1 for ~ 15 h. The cells were then heat shocked in a water bath at 44°C for 20, 30, and 40 min. Twelve hours after heat shock, 0.94 mg/ml of *D*-luciferin ($100 \mu\text{l}$) was added to each well. The cells were then incubated for 1 min prior to BLI. Immediately after the last imaging point, an ELISA for the actual hsp70 protein levels was conducted on each sample.

3.7 Colocalization of hsp70 on Laser-Irradiated Raft Cultures

The immunohistochemistry of the raft cultures is shown in Figs. 8(a)–8(e). Figure 8(a) shows the (H&E) stain of a normal untreated raft at a $20\times$ magnification, the epithelial and stromal layers can be clearly identified. Figure 8(b) shows the H&E of a raft that has been irradiated with the CO_2 laser (1.584 W/cm^2) at a $40\times$ magnification. We observe that the epithelial layer is thermally damaged and appears to be coagulated. Figure 8(c) shows a Gomori trichrome stain, which stains for connective tissue, of the same raft as in Fig. 8(b) at

a $40\times$ magnification. The blank spot on the Gomori trichrome stain reveals that connective tissue is ablated due to the lasing process. Figure 8(d) shows the hsp70 antibody stain of a raft culture irradiated with the CO_2 laser for 1.584 W/cm^2 for 60 s ($40\times$). A red dotted line drawn $\sim 170 \mu\text{m}$ below the surface, demarcates the region where maximal hsp70 expression is observed. The insert in Fig. 8(e) shows Fig. 8(d) at $100\times$ magnification. Figure 8(f) shows the bioluminescent microscopy image. The laser irradiated rafts emit maximal bioluminescence 150 to $200 \mu\text{m}$ below the surface of the raft. This region of maximal expression corre-

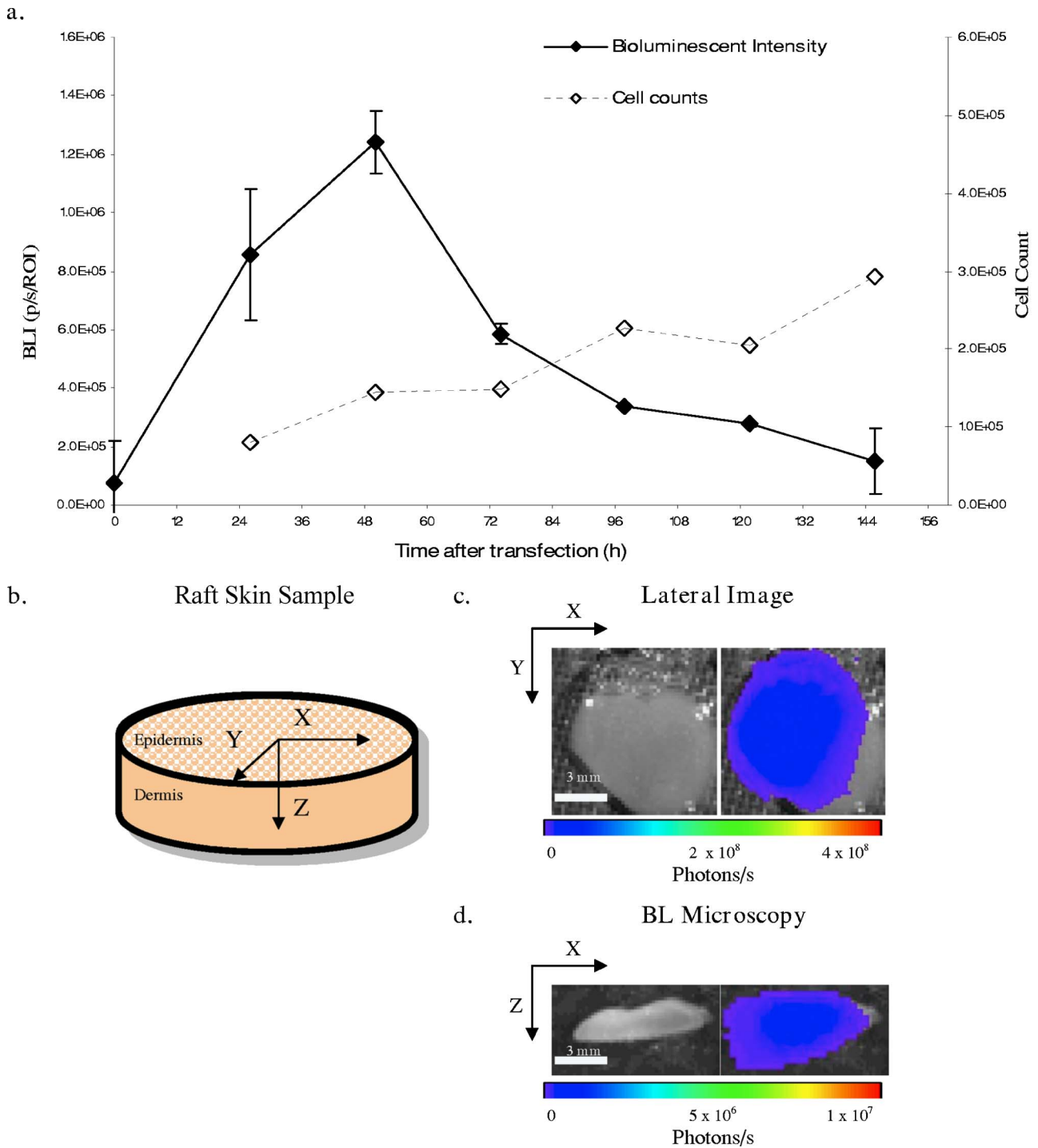


Fig. 6 Transient transfection kinetics and the efficacy of *in situ* transfections. (a) Bioluminescent light intensity and cell counts for adenovirally (Ad-hsp70-luc) transfected normal human dermal fibroblasts are plotted versus time. The bioluminescent intensity sharply increased from 0 to 49 h and plummeted from 49 to 145 h. At 145 h, the signal decreased to less than 17% of the initial signal. At time=-24 h, 7 six-well plates were seeded with NHDFs at a concentration of 9.6×10^4 cells per well. At time=0, all 7 plates were then transfected with $20 \mu\text{l}$ of adenovirus (titer= 1.3×10^7 PFU/ml, MOI=1). After transfection at time=15 h, the first plate of NHDFs was heated in a water bath at 44°C for 40 min. At time=25 h, $100 \mu\text{l}$ of 0.94 mg/ml of luciferin was added 3 min prior to BLI. Plates 2, 3, 4, 5, 6, and 7 were heated at time=15, 39, 63, 87, 111, or 135 h, respectively. The plates were then imaged at time=25, 49, 73, 97, 121, and 145 h. Values are reported as mean standard deviation; error bars smaller than symbol are not shown. (b) Visual representation of raft imaging dimensions (c) Lateral bioluminescent image (IVIS 200). (d) Bioluminescent microscopy image (IVIS 200). In order to assess the transfection efficiency in three dimensions, independent of heating, the Ad-CMV-luc-IRES2-eGFP with a MOI of 1 was used to transfect the rafts.

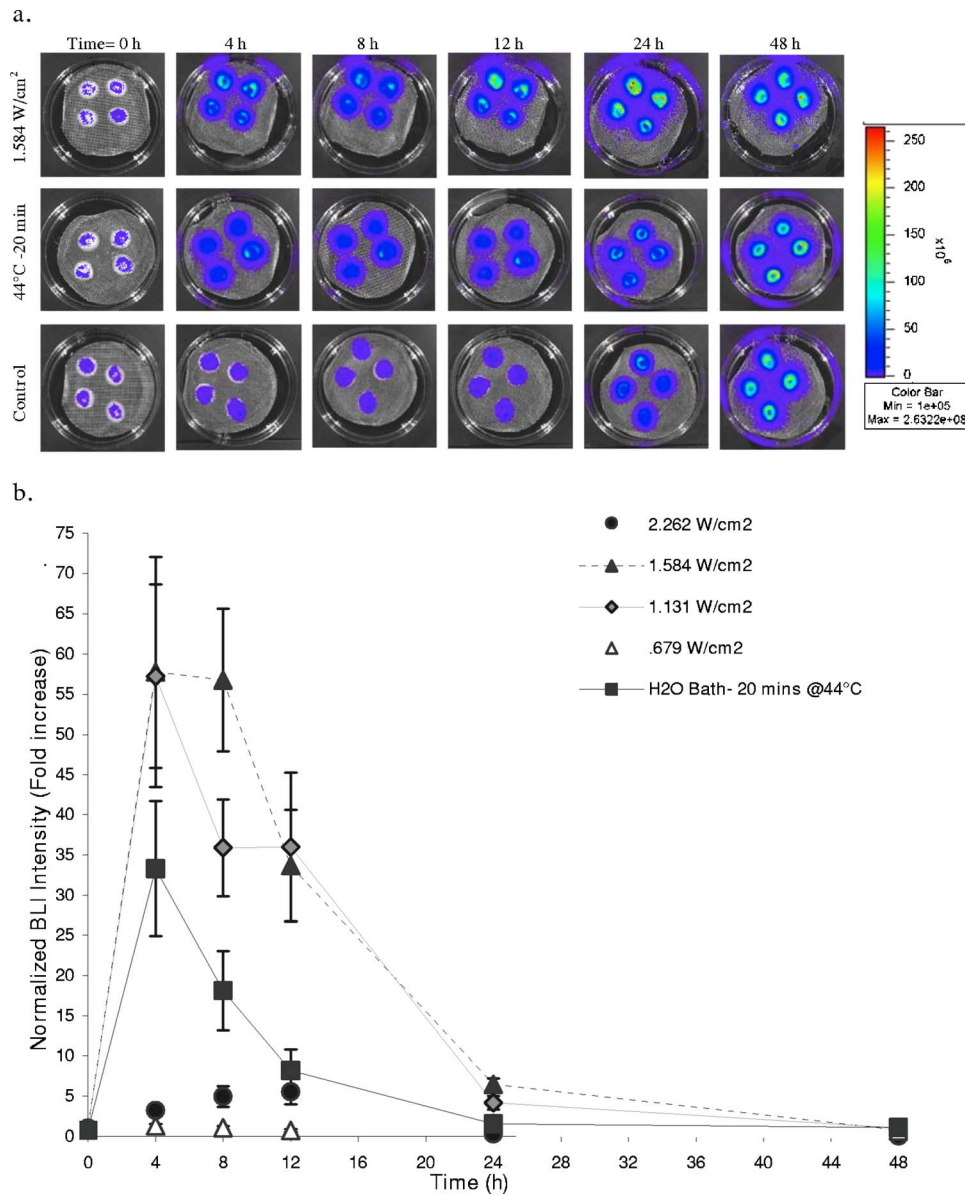


Fig. 7 Visualizing the induction of hsp70 in organotypic raft cultures using BLI. (a) The pseudocolor graphic of the bioluminescent signal of three samples of raft cultures: 1.584 W/cm² (0.72 W), 44°C for 20 min, and unheated control is shown for visualization. The pseudocolor of the plot indicates where the highest light emission is present (red - color online only). At $t=-15$ h, 28 rafts were transfected with adenovirus (hsp70-luc) with MOI=1. At $t=0$ h, the rafts were exposed to heat shock inducing conditions via a water bath and CO₂ laser radiation. The 28 total rafts were treated in the following manner: two negative control groups ($n=4$), a positive control 44°C for 20 min ($n=4$), 0.679 W/cm² for 1 min ($n=4$), 1.131 W/cm² for 1 min ($n=4$), 1.584 W/cm² for 1 min ($n=4$), and 2.262 W/cm² for 1 min ($n=4$). After heat shock, 200 μ l of 0.94 mg/ml of luciferin (Biosynth AG) was applied directly on top of each raft and allowed to diffuse within the raft for 1 min before imaging. The samples were then imaged for 1 min with the IVIS 100 system at $t=0, 4, 8, 12, 24,$ and 48 h. (b) A plot of the intensity of the bioluminescent signal over time in adenovirally transfected raft cultures. For all laser radiated samples, the maximal expression occurred at $t=4$ to 8 h after exposure. Maximal expression occurred at $t=4$ h for the rafts heated in a water bath. The rafts exposed to 0.72 W (1.584 W/cm²) had the highest bioluminescence expression. The data was normalized to the bioluminescent intensity of the control rafts (not heated), and the means and standard deviations were plotted. Values are reported as mean standard errors; error bars smaller than symbol are not shown.

sponds to the same area denoted by the dotted red line in Fig. 8(d) where maximum hsp70 protein levels were located.

4 Discussion

In this study, we demonstrated that an organotypic raft culture model equipped with a bioluminescent reporter gene, under control of a heat activated promoter (hsp70a1), can be used to

monitor thermally modulated gene expression. This approach provides a model capable of noninvasively detecting subtle biochemical changes of biological processes demanding sequential analysis, as in laser-tissue damage studies. An inducible and highly characterized protein, hsp70, was tested in the context of this novel model. An adenovirus (hsp70a1-luc) equipped with the hsp70 promoter is shown to efficiently

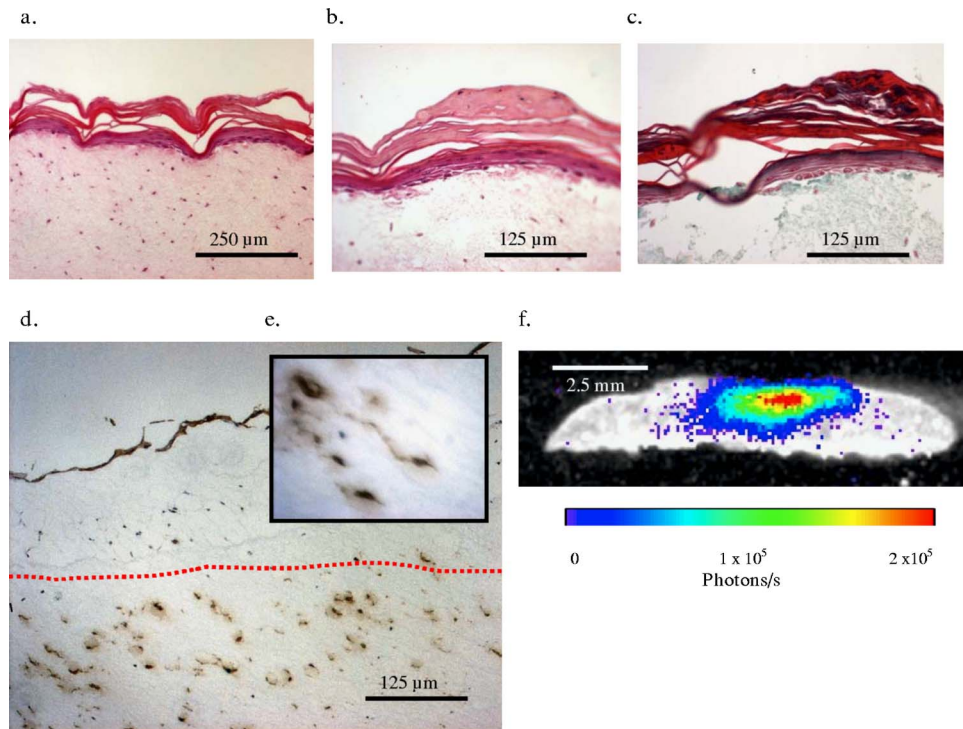


Fig. 8 Immunohistochemistry of raft cultures. (a) H&E stain of a normal raft at 20 \times magnification. (b) H&E stain of a raft irradiated with a CO₂ laser for 1.584 W/cm² for 60 s (40 \times magnification, bar, 125 μ m). (c) Gomori trichrome (green) of the same raft in (b). (d) Hsp70 antibody staining of a laser irradiated raft taken at 40 \times magnification. (e) 100 \times magnification of slide (d). (f) Bioluminescent microscopy of 96- μ m thick cross-section slice of laser damaged raft imaged with IVIS 200 (1.584 W/cm², 1.0 W, for 60 s).

transfect differentiated raft cultures *in situ* and permitted hsp70 transcription to be monitored after laser radiation [Figs. 7(a) and 7(b)]. The results indicate that hsp70 expression is maximal 4 to 12 h after laser radiation. These findings are consistent with previous studies on hsp70 expression.^{12,13} The results of the CO₂ laser-radiated rafts reveal that a minimum radiation of 0.679 W/cm² was needed to activate the hsp70 response, and a maximum radiation of 2.262 W/cm² was associated with tissue ablation and significant cell death.

Although the utility of this model is shown in the context of a laser-tissue interaction, it is noteworthy to mention its potential utility beyond this application. For instance, this model can be used to study wound repair processes, or in any other pathological milieu which require monitoring of biomolecular relationships. This model is quite versatile, since the skin constituents and its environment can be selected and controlled by the user. Thus, this approach can be used to create models for other tissues of interest. Also, the model can be further expanded to study other genes of interest, such as TGF- β 1 and TGF- β 3, which have been identified to play roles in wound repair.^{5,29,31}

4.1 Characterizing the hsp70 Response

4.1.1 Using BL as a surrogate marker for hsp70 mRNA and protein

After identifying that a MOI=1 resulted in optimal transfection, the correlation between bioluminescence and hsp70 protein and mRNA levels was determined. The data shows that increasing the heat shock exposure causes increases in biolu-

minescent light intensity, native hsp70 protein levels, and hsp70 mRNA levels [Figs. 2, 3(d), and 4(a)–4(c)]. Heat shocking the NHDFs in a water bath at 44 $^{\circ}$ C for 10 min results in a 25-fold increase in bioluminescent intensity and a 12-fold increase in hsp70 mRNA levels compared to the controls. Exposing the NHDFs to 44 $^{\circ}$ C for 20 and 40 min results in 100- and 130-fold increases in bioluminescent intensity, 4- and 8-fold increases in native hsp70 protein levels, and 200- and 500-fold increases in hsp70 mRNA expression, respectively [Figs. 2, 3(d), and 4(a)–4(c)]. Plotting these bioluminescent intensities versus the hsp70 mRNA (data not shown) and native hsp70 protein levels (ELISA) [Fig.3(d)], generates correlation coefficients of ($R^2=0.91$) and ($R^2=0.99$), respectively. Thus, the data indicates that the absolute bioluminescence intensity is an accurate surrogate marker for actual hsp70 levels, as well as for relative hsp70 mRNA levels.

4.1.2 Temporal features of the hsp70 response

This study not only served to verify the hsp70 system was sensitive to minor temperature changes, but also revealed some significant temporal information about the hsp70 response. The most interesting temporal finding for the NHDFs is that the maximal hsp70 mRNA levels occurred 4 to 6 h after heat shock, while maximal bioluminescent intensity occurred 6 to 12 h after heat shock [Figs. 2 and 4(a)]. This 6 to 12 h bioluminescent peak corresponds to the time of maximal hsp70 expression. This bioluminescent intensity peak agrees with previous literature where maximal expression was found to occur 6 to 12 h after heat shock induction.¹³ The observed

decrease in hsp70 mRNA levels 8 to 12 h post-heat shock may be the result of negative feedback regulation caused by increased hsp70 protein levels. This theory is corroborated by the increasing bioluminescence intensity between 8 to 12 h. Moreover, the 2-h delay between the hsp70 mRNA peak and bioluminescence intensity maximum is an indication of the time it takes to translate mRNA into nascent protein.

4.1.3 Crossing physiologic zones of stress

In previously published hsp70 studies, five zones of physiologic stress were defined.¹² In this study, the real-time RT-PCR and the bioluminescent intensity data served to verify the crossing of one of these physiologic zones. O'Connell-Rodwell et al. characterized zone 3 where times and/or temperatures of stress resulted in delayed peaks of expression.¹² The data indicates that zone 3 was traversed as the cell's heat shock exposure was prolonged from 44°C for 10 min to 44°C for 20 min. Crossing this boundary resulted in 4 times higher bioluminescent intensity, 20 times higher hsp70 mRNA levels, and a delayed hsp70 response [Figs. 2 and 4(a)]. This delayed hsp70 response is clearly demonstrated using the bioluminescence data where the maximal bioluminescent intensity occurred at 4 to 6 h for the 10 min exposure and at 12 h for the 20 min heat shock [Fig. 2]. Adhering to the delayed hsp70 response theory, the hsp70 mRNA data demonstrated that the response to the 10 min exposure was maximal 0 to 4 h after heat shock, and the response to the 20 min exposure peaked at 4 to 6 h after heat shock [Fig. 4(a)].

Overall, the results indicated that our system is sensitive to detect increases in heat shock. From the literature and previous studies, we expected the hsp70 response to behave as many other proteins do in that it would be upregulated after an initial stimulus and then decline after the stimulus had been removed.¹³ When a cell is exposed to thermal stress (via heated water bath or laser radiation) a multitude of proteins denature. Protein denaturation is characterized by alterations in the secondary and tertiary structure of the molecule. The proteins loss of structure precipitates its loss of function. The presence of denatured proteins within the cell acts as a stimulus for the transcription of hsp70. Once sufficient hsp70 protein has been translated for repair, the additional hsp70 can bind the heat shock transcription factor, HSF1, which then downregulates hsp70 production. Figure 2 shows that increasing the exposure time at 44°C from 20 to 40 min leads to an increase in hsp70 promoter activation and more bioluminescent light intensity. The NHDFs are incubated at 37°C thus when exposed to the 44°C water bath, they undergo a 7°C temperature increase. This increase agrees with previous literature where moderate heat shock temperatures (39 to 44°C) were used to activate the heat shock response.^{32,33} As anticipated, increasing the duration of heat shock exposure from 20 to 40 min enhanced the degree of activation of the heat shock response.

4.2 Transient Transfection of NHDFs

The transient nature of adenoviral transfection precludes the transfection of cells prior to constructing skin equivalents [Fig. 6(a)]. The data illustrates that a peak in bioluminescent intensity is observed 48 h after transfection. The data reveals

that the bioluminescent intensity is lower at 24 h after transfection than at 48 h. This lower bioluminescent intensity could be due to an incubation time. In essence, this could be related to the time required for the adenovirus to become familiar with the cell's transcriptional machinery. In previous adenovirus studies, Kugel identified an early transition in RNA polymerase II transcription, termed "escape commitment." Escape commitment occurs rapidly after initiation and is characterized by sensitivity to competitor DNA.³⁴ This competitor DNA may be the reason for the cell's low bioluminescent intensity 24 h posttransfection.³⁴ The cells may not be fully functioning as far as transgene expression goes until ~48 h, thus explaining the maximum bioluminescent expression occurring 48 h after transfection. From 49 to 73 h, the bioluminescent signal decreases by 50% and by 145 h only 17% of the initial signal remains [Fig. 6(a)]. The transgene expression decreases due to cell proliferation and cell expulsion of adenoviral DNA. Because half of the bioluminescent signal is present 72 h after transfection, this can be noted as an end point for adenovirus experimentation. Thus, the window for experimentation using this adenovirus ranges from 24 to 60 h after transfection. This has important implications for the transfection of rafts. Because rafts take 10 to 14 days to fully develop, transfecting the cells before raft construction is not feasible. As a direct ramification of these findings, the rafts were transfected *in situ* after being fully developed. Of concern is the fact that *in situ* transfection of intact rafts may not yield spatially homogeneous transfection. The results of the experiments conducted with the constitutively expressed Ad-CMV-luc-IRES2-eGFP, show a relatively uniform BL intensity (both in the *xy* and *xz* planes) indicating that the *in situ* transfection of the rafts did not result in a gradient of transfection efficiency. Thus, *in situ* transfections are a suitable and effective method for transfecting intact rafts [Figs. 6(c) and 6(d)].

4.3 Cell-Type Dependent hsp70 Expression

After characterizing the hsp70 response in fibroblasts, the hsp70 response was examined in the other cell populations present in skin raft cultures. MOI optimization experiments were conducted for the NHDFs, NHEKs, and NHEMs and the MOI=1 was optimal for all cell lines (data not shown). The cells were transfected with the adenovirus (MOI=1) and their heat shock response was observed. Interestingly, the various cell types illustrated different hsp70 response kinetics following heat shock induction [Figs. 5(a) and 5(b)]. The variation between the cell lines could be due to differences in transfection efficiency or to differences in the cellular stress response. Figures 5(a) and 5(b) show that for the same MOI and heating exposure time, the NHEKs have a 10-fold increase in bioluminescent intensity while having slightly lower native hsp70 protein concentrations. The reason for this may be due to impaired adenovirus transfection. In previous studies, the receptor integrin $\alpha(V)\beta(3)$ was implicated in increased adenovirus transfection.³⁵ NHEKs may elicit a higher bioluminescent signal due to increased affinity to upregulate the integrin $\alpha(V)\beta(3)$ receptor. Besides the integrin receptor, other studies have observed that hsp70 is constitutively expressed in normal skin cells, with the highest level being observed in the NHEKs.^{36,37} Thus, because the NHEKs have higher expres-

sion before induction, this increased basal activity may result in higher expression after heat shock induction.

4.3.1 NHEM apoptotic activity

NHEMs reacted much differently than the other cell lines. While increasing the duration of heat shock exposure led to an increase in bioluminescent intensity [Fig. 5(b)], it resulted in decreased hsp70 protein levels for the NHEMs in contrast to the NHEKs and NHDFs [Fig. 5(a)]. The flow cytometry results indicate that this may be due to significant apoptosis occurring in the NHEMs [Fig. 3(i)]. Using flow cytometry, the JC-1 assay was employed to determine the cell's apoptotic activity. In Figs. 3(g)–3(i), the JC-1 assay data revealed that for the NHDFs and the NHEKs less than 30% of the cells were apoptotic, regardless of the heating protocol, yet for the NHEMs >60% of the cells, including the unheated controls, were apoptotic. These findings are not unusual, other studies have shown that NHEMs are notoriously difficult to culture and are prone to undergo apoptosis.³⁸ Due to the significant apoptotic activity of the NHEMs, they were not used in the construction of the raft cultures.

4.4 Efficacy and Utility of Organotypic Raft Culture Model

4.4.1 Inducing hsp70 expression on rafts with a heated water bath

Before laser radiation experiments were performed, transfected rafts were tested using a heated water bath. The rafts were moderately heat shocked at 44°C for 20 min. Bioluminescent signals indicated that the peak hsp70 expression occurred 4 h post-heat shock [Fig. 7(b)]. This finding is consistent with previous cell culture studies, which also found that hsp70 expresses maximally 4 h after exposure to heat shock.¹³ The rafts exposed to moderate heat shock conditions then decreased hsp70 expression after peak expression at 4 h. This decreased expression was anticipated due to negative feedback provided by HSF1 and is consistent with previous findings.¹³

4.4.2 Laser irradiation of raft cultures

In order to determine the powers for the laser-radiation experiments, a thermocouple was utilized to determine the temperature increases at various powers (data not shown). Irradiances of 1.131 W/cm² for 60 s correlated to a maximum temperature rise of ~22°C at 500 μm below the surface of the raft. This is significantly higher than the 7°C temperature rise in the water bath. However, given that protein denaturation is a rate process, it is expected that a reduction in the time of heating (60 s versus 20 min) will permit higher tolerable temperature values while generating a similar response.

Our results show that in the raft models, increasing the laser irradiance results in increased normalized bioluminescent intensity [Fig. 7(b)]. Thus, for increased irradiances, an increased amount of hsp70 expression is observed. (Note that the irradiance of 2.262 W/cm² resulted in a significantly lower signal as greater than 70% of the tissue was ablated.) The data also showed that when increasing the irradiance from 1.131 to 1.584 W/cm², a comparably bioluminescent peak is seen at 8 h. This correlates with previous studies that indicate that under moderate heat shock conditions, a maxi-

mal hsp70 response is seen sooner after induction.¹³ Since the higher irradiance would result in increased heat shock conditions, this prolonged hsp70 transcription is anticipated. The raft that is exposed to a higher irradiance would presumably undergo a more severe heat shock, resulting in more protein denaturation. This increases the amount of HSF1 that is freely available and results in increased promoter activation on the heat shock element. Another interesting finding is the raft exposed to the irradiance of 0.679 W/cm² experienced minimal damage and likewise elicited minimal heat shock response. This irradiance sets the lower boundary on eliciting the heat shock response. Thus, a window for CO₂ laser radiation activation of the hsp70 response was found in this study to fall within the range of 0.679 to 2.262 W/cm² for 60-s exposures.

In order to ensure that the bioluminescent intensity accurately reflected regions where hsp70 expression was most substantial, bioluminescent microscopy was compared with hsp70 antibody staining. The radiated rafts had the most substantial hsp70 antibody staining (the red line) at a depth of ~150 μm [Fig. 8(d)]. This region corresponded exactly to the region where the highest bioluminescence intensity (red region) was observed [Fig. 8(f)]. These results confirmed our findings that our adenovirally transfected skin model is capable of accurately detecting subtle biochemical changes using BLI.

5 Conclusion

We present an organotypic raft model used in combination with BLI techniques. The efficacy of the raft model was validated and characterized by investigating the role of hsp70 as a sensitive marker of thermal damage. BLI indicated that peak hsp70 expression occurs 4 to 12 h after exposure to thermal stress conditions. The findings suggest a minimum radiation of 0.679 W/cm² was needed to activate the hsp70 response, and a higher radiation of 2.262 W/cm² was associated with a severe reduction in hsp70 response due to tissue ablation. Real-time RT-PCR and ELISA protein assays confirmed that BLI was an accurate surrogate for actual hsp70 protein levels and hsp70 mRNA levels present in the cells. The temporal features of the real-time RT-PCR and BLI peak values were found to be useful in evaluating the crossing of physiological stress zones. Hsp70 expression was localized in the damaged tissue region using bioluminescent microscopy studies. These results indicate that quantitative BLI in engineered tissue equivalents provides a powerful model that enables longitudinal studies of gene expression. Such a model can be used as a high throughput screening platform in studies of laser interaction with dermal tissue.

Acknowledgments

The authors wish to thank the following individuals who provided expert technical support. Dr. Lillian Nanney for her immunohistochemistry expertise. Connie Nixon, from the SDRC Tissue Culture Core, for providing our cell lines and guidance with our *in vitro* analysis. Kelly Parman, from the SDRC Immunohistochemistry Core for the hsp70 immunolocalization. Evelyn Okediji for her histology expertise. Dr. Rick Haselton for use of his cell culture facility and assistance. These studies were supported by a National Institute of

Health pilot and feasibility grant (No. P30-AR41943) from the Skin Disease Research Core Center (SDRCC) and a Department of Defense Medical Free Electron Laser (MFEL) program grants (No. F49620-01-1-0429 and (No. FA9550-04-1-0045).

References

1. S. Thomsen, "Pathologic analysis of photothermal and photomechanical effects of laser-tissue interactions," *Photochem. Photobiol.* **53**(6), 825–835 (1991).
2. S. Thomsen, J. A. Pearce, and W. F. Cheong, "Changes in birefringence as markers of thermal damage in tissues," *IEEE Trans. Biomed. Eng.* **36**(12), 1174–1179 (1989).
3. N. Wu et al., "Real-time visualization of MMP-13 promoter activity in transgenic mice," *Matrix Biol.* **21**(2), 149–161 (2002).
4. N. Wu, E. D. Jansen, and J. M. Davidson, "Comparison of mouse matrix metalloproteinase 13 expression in free-electron laser and scalpel incisions during wound healing," *J. Invest. Dermatol.* **121**(4), 926–932 (2003).
5. A. Capon and S. Mordon, "Can thermal lasers promote skin wound healing?," *Am. J. Clin. Dermatol.* **4**(1), 1–12 (2003).
6. T. Desmettre, C. A. Maurage, and S. Mordon, "Heat shock protein hyperexpression on chorioretinal layers after transpupillary thermotherapy," *Invest. Ophthalmol. Visual Sci.* **42**(12), 2976–2980 (2001).
7. B. Laxman et al., "Noninvasive real-time imaging of apoptosis," *Proc. Natl. Acad. Sci. U.S.A.* **99**(26), 16551–16555 (2002).
8. J. Virostko et al., "Factors influencing quantification of in vivo bioluminescence imaging: application to assessment of pancreatic islet transplants," *Mol. Imaging* **3**(4), 333–342 (2004).
9. C. H. Contag and M. H. Bachmann, "Advances in in vivo bioluminescence imaging of gene expression," *Annu. Rev. Biomed. Eng.* **4**, 235–260 (2002).
10. Y. Shi et al., "CARP, a cardiac ankyrin repeat protein, is up-regulated during wound healing and induces angiogenesis in experimental granulation tissue," *Am. J. Pathol.* **166**(1), 303–312 (2005).
11. R. I. Morimoto, P. E. Kroeger, and J. J. Cotto, "The transcriptional regulation of heat shock genes: a plethora of heat shock factors and regulatory conditions," *EXS* **77**, 139–163 (1996).
12. C. E. O'Connell-Rodwell et al., "A genetic reporter of thermal stress defines physiologic zones over a defined temperature range," *FASEB J.* **18**(2), 264–271 (2004).
13. J. T. Beckham et al., "Assessment of cellular response to thermal laser injury through bioluminescence imaging of heat shock protein 70," *Photochem. Photobiol.* **79**(1), 76–85 (2004).
14. A. G. Pockley, "Heat shock proteins, inflammation, and cardiovascular disease," *Circulation* **105**(8), 1012–1017 (2002).
15. B. Kao et al., "Evaluation of cryogen spray cooling exposure on in vitro model human skin," *Lasers Surg. Med.* **34**(2), 146–154 (2004).
16. B. Kao et al., "Novel model for evaluation of epidermal preservation and dermal collagen remodeling following photorejuvenation of human skin," *Lasers Surg. Med.* **32**(2), 115–119 (2003).
17. A. Capon et al., "Laser assisted skin closure (LASC) by using a 815-nm diode-laser system accelerates and improves wound healing," *Lasers Surg. Med.* **28**(2), 168–175 (2001).
18. J. M. Davidson, "Animal models for wound repair," *Arch. Dermatol. Res.* **290**, S1–S11 (1998).
19. E. V. Ross et al., "Nonablative skin remodeling: selective dermal heating with a mid-infrared laser and contact cooling combination," *Lasers Surg. Med.* **26**, 2, 186–195 (2000).
20. M. J. Bissell, H. G. Hall, and G. Parry, "How does the extracellular matrix direct gene expression?," *J. Theor. Biol.* **99**(1), 31–68 (1982).
21. A. R. Viehoveer et al., "Organotypic raft cultures as an effective in vitro tool for understanding Raman spectral analysis of tissue," *Photochem. Photobiol.* **78**(5), 517–524 (2003).
22. D. Asselineau et al., "Human epidermis reconstructed by culture: is it "normal"?," *J. Invest. Dermatol.* **86**(2), 181–186 (1986).
23. E. Papadavid and A. Katsambas, "Lasers for facial rejuvenation: a review," *Int. J. Dermatol.* **42**(6), 480–487 (2003).
24. E. V. Ross, J. R. McKinlay, and R. R. Anderson, "Why does carbon dioxide resurfacing work?," *Basal Facts* **135**(4), 444–454 (1999).
25. A. Vogel and V. Venugopalan, "Mechanisms of pulsed laser ablation of biological tissues," *Chem. Rev. (Washington, D.C.)* **103**(2), 577–644 (2003).
26. C. Hunt and S. Calderwood, "Characterization and sequence of a mouse hsp70 gene and its expression in mouse cell lines," *Gene* **87**(2), 199–204 (1990).
27. B. Baggett et al., "Thermostability of firefly luciferases affects efficiency of detection by in vivo bioluminescence," *Mol. Imaging* **3**(4), 324–332 (2004).
28. *User Bulletin #2: ABI Prism 7700 Sequence Detection System*, Applied Biosystems, Foster City, CA (2001).
29. D. J. Whitby and M. W. Ferguson, "Immunohistochemical localization of growth factors in fetal wound healing," *Dev. Biol.* **147**(1), 207–215 (1991).
30. R. A. Russell et al., "Transient foamy virus vector production by adenovirus vectors," *Gene Ther.* **11**(3), 310–316 (2004).
31. P. Martin, "Wound healing—aiming for perfect skin regeneration," *Science* **276**(5309), 75–81 (1997).
32. L. Huang, N. F. Mivechi, and D. Moskophidis, "Insights into regulation and function of the major stress-induced hsp70 molecular chaperone in vivo: analysis of mice with targeted gene disruption of the hsp70.1 or hsp70.3 gene," *Mol. Cell. Biol.* **21**(24), 8575–8591 (2001).
33. A. Y. Liu et al., "Transient cold shock induces the heat shock response upon recovery at 37 degrees C in human cells," *J. Biol. Chem.* **269**(20), 14768–14775 (1994).
34. J. F. Kugel and J. A. Goodrich, "A kinetic model for the early steps of RNA synthesis by human RNA polymerase II," *J. Biol. Chem.* **275**(51), 40483–40491 (2000).
35. N. Pampori et al., "Mechanisms and consequences of affinity modulation of integrin alpha(V)beta(3) detected with a novel patch-engineered monovalent ligand," *J. Biol. Chem.* **274**(31), 21609–21616 (1999).
36. F. Trautinger et al., "Human keratinocytes in vivo and in vitro constitutively express the 72-kD heat shock protein," *J. Invest. Dermatol.* **101**(3), 334–338 (1993).
37. E. Souil et al., "Treatment with 815-nm diode laser induces long-lasting expression of 72-kDa heat shock protein in normal rat skin," *Br. J. Dermatol.* **144**(2), 260–266 (2001).
38. T. Alanko, M. Rosenberg, and O. Saksela, "FGF expression allows nevus cells to survive in three-dimensional collagen gel under conditions that induce apoptosis in normal human melanocytes," *J. Invest. Dermatol.* **113**, 1, 111–116 (1999).